LA-UR-00-1067

Title: **^{7}Li(p,n) Nuclear Data Library for Incident Proton Energies to 150 MeV**

Author(s): S. G. Mashnik, M. B. Chadwick, P. G. Young, R. E. MacFarlane, and L. S. Waters

Submitted to:

http://lib-www.lanl.gov/la-pubs/00393814.pdf

^{7}Li(p,n) Nuclear Data Library for Incident Proton Energies to 150 MeV

S. G. Mashnik, M. B. Chadwick, P. G. Young, R. E. MacFarlane, and L. S. Waters
Los Alamos National Laboratory, Los Alamos, NM 87545

Abstract

Researchers at Los Alamos National Laboratory are considering the possibility of using the Low Energy Demonstration Accelerator (LEDA), constructed at LANSCE for the Accelerator Production of Tritium program (APT), as a neutron source. Evaluated nuclear data are needed for the p+^{7}Li reaction, to predict neutron production from thin and thick lithium targets. In this report we describe evaluation methods that make use of experimental data, and nuclear model calculations, to develop an ENDF-formatted data library for incident protons with energies up to 150 MeV. The important ^{7}Li(p,n$_0$) and ^{7}Li(p,n$_1$) reactions are evaluated from the experimental data, with their angular distributions represented using Lengendre polynomial expansions. The decay of the remaining reaction flux is estimated from GNASH nuclear model calculations. This leads to the emission of lower-energy neutrons and other charged particles and gamma-rays from preequilibrium and compound nucleus decay processes.

The evaluated ENDF-data are described in detail, and illustrated in numerous figures. These data need to be tested through use in radiation transport simulations of thin and thick lithium targets bombarded by protons.

I. INTRODUCTION

As a part of the Accelerator Production of Tritium (APT) Project [1], the Low Energy Demonstration Accelerator (LEDA) has been constructed at the Los Alamos Neutron Science Center [2]. LEDA is a high-current low-energy proton accelerator that can be used to provide a source of neutrons, following proton bombardment on suitable targets. For instance, high-Z targets can be used to produce spallation neutrons. However, there is a recent interest in the use of a ^{7}Li target, which, when bombarded with protons, can produce a relatively high yield of quasimonoenergetic neutrons in the forward direction via the ^{7}Li(p,n) reaction. In particular, this reaction may be useful to provide neutrons with energies near 14 MeV, for materials testing for the fusion program.

In addition to the above application, quasimonoenergetic and broad neutron sources are needed for research in other areas in nuclear science and technology, *e.g.* accelerator-transmutation of waste (ATW), radiation damage studies, medical isotope production, and physics cross section experiments.

In order to assess the feasibility of using a lithium target to produce neutrons, accurate evaluated cross section data are needed. These data can be used to predict the neutron yield, as well as the neutron energy and angular dependencies, from both thin and thick targets. (Thin targets allow the possibility of producing quasimonoenergetic neutron sources[1], whereas thicker targets produce broad-spectrum neutron sources.)

This report is organized as follows. Section II provides an overview of reactions that can be used to provide neutron sources, and Section III summarizes measured data available for the ^{7}Li(p,n) reaction. These data include both high-energy neutrons that populate the ground-state and first excited state of ^{7}Be, as well as lower energy neutrons from the excitation of other beryllium states, and continuum neutrons from break-up reactions. Section IV describes our evaluation methods, based on use of experimental data as well as nuclear model calculations. In Section V we provide some figures that illustrate certain features of the evaluated ENDF data. Our conclusions and directions for future work are given in Section VI.

II. BACKGROUND: QUASIMONOENERGETIC NEUTRON SOURCES

Usually, charged-particle reactions of the type (p/d/t) + $A \rightarrow$ n+$B + Q$ are used for the production of fast quasimonoenergetic neutrons; here, A is a light-weight nucleus, B is the residual nucleus, and the energy release Q value can be positive or negative.

Only neutron emission forward with respect to the charged-particle beam is of interest, since: 1) the neutron yield is forward peaked, 2) neutron emitted at 0 deg have the highest energy, 3) these neutrons are certainly unpolarized.

For comparison, Table I shows the relevant kinematic information for a number of potential reactions as monoenergetic neutron sources presented by Drosg in Ref. [3].

[1] Though our results shown in this paper indicate that once the incident proton energy exceeds a few-MeV, even thin targets result in a substantial number of lower-energy neutrons.

TABLE I

Projectile Threshold Energies and Neutron Energies at 0 deg in the Laboratory System for the Ground State Reaction, $E_{n0}(0)$, for 180 deg, $E_{n0}(180)$, and for the Breakup Reaction, E_{nBR}, at the Threshold (adapted from Drosg [3])

#	Reaction	Threshold	(MeV)	$E_{n0}(0)$ (Mev)	$E_{n0}(180)$ (Mev)	E_{nBR} (MeV)
1	^{2}H(d,n)^{3}He	Ground state	0.0	2.449		
		Breakup	4.451	7.706		0.578
2	^{3}H(d,n)^{4}He	Ground state	0.0	4.029		
		Breakup	3.711	20.461		0.305
3	^{2}H(t,n)^{4}He	Ground state	0.0	4.029		
		Breakup	5.558	23.007		0.690
4	^{3}H(p,n)^{3}He	Ground state	1.019	0.064	0.064	
		Breakup	8.355	7.585		0.552
5	^{7}Li(p,n)^{7}Be	Ground state	1.881	0.030	0.030	
		1st excited state	2.372	0.650		
		Breakup	3.697	2.016		0.059
6	^{11}B(p,n)^{11}C	Ground state	3.018	0.021	0.021	
		1st excited state	5.202	2.388		
		Breakup	11.256	8.473		0.081
7	^{1}H(t,n)^{3}He	Ground state	3.051	0.573	0.573	
		Breakup	25.011	17.639	0.019	4.702
8	^{1}H(^{7}Li,n)^{7}Be	Ground state	13.097	1.440	1.440	
		1st excited state	16.514	3.842	0.540	
		Breakup	25.742	8.188	0.254	2.833
9	^{1}H(^{11}B,n)^{11}C	Ground state	32.980	2.537	2.537	
		1st excited state	56.842	11.880	0.542	
		Breakup	122.998	32.661	0.198	9.456
10	^{1}H(^{13}C,n)^{13}N	Ground state	41.769	2.791	2.791	
		Breakup	68.798	12.175	0.641	4.605
11	^{1}H(^{15}N,n)^{15}O	Ground state	56.199	3.319	3.319	
		1st excited state	138.580	25.726	0.430	
		Breakup	172.181	33.815	0.327	10.175

Only reactions # 4, 5, and 6 are relevant for LEDA which accelerates protons. Note that a strong limitation on neutron source properties comes from the target construction.

An ideal target should be isotopically pure and self-supporting: otherwise, the specific neutron yield will be lower because of a lower areal density of the target material, and the additives will increase the energy spread, further reducing the specific neutron yield.

For the p+^{7}Li (#5) and p+^{11}B (#6) reactions, isotopically pure solid targets are possible. Usually they have a backing with good thermal conductivity (preferably tantalum) that serves as a beam stop and allows beam power removal by means of an air jet or a water spray.

The ^{11}B(p,n)^{11}C (#6) reaction has a number of advantages [3] compared to the ^{7}Li(p,n)^{7}Be: 1) a smaller minimum energy, 2) a smaller kinetic energy spread, 3) a better intrinsic energy resolution (higher threshold), 4) a much wider monoenergetic energy range. However, the specific yield is typically a factor of 5 lower than for p+^{7}Li, and, furthermore, ^{11}B targets are more difficult to produce than ^{7}Li targets. Therefore this source has not been used much up to now. Further details and references can be found in [3].

The advantages of the p+^{7}Li reaction as a neutron source are the following [3]: 1) Small kinematic energy spread inside of an opening angle; e.g., for an opening angle of ± 5 deg, the kinematic spread is only of about 0.15% (see, Fig. 3 in [3]). 2) Between 0.4– and 0.7–MeV neutron energy, the yield is higher than for the competing reaction p+^{3}H (#4). An additional advantage over the p+^{3}H reaction is the higher projectile energy that gives better time resolution in TOF experiments. 3) The production of targets is comparatively simple. They usually consist of lithium metal evaporated on a tantalum backing. Even natural lithium can be used [the (p,n) threshold of ^{6}Li at 5.92 MeV is outside the useful range of the p+^{7}Li reaction].

Lithium-metal targets are easily and inexpensively prepared, require no elaborate safety precautions in handling before bombardment, and provide a relatively intense neutron source when bombarded by protons with energies exceeding $E_p = 1.880612 \pm 0.00009$ MeV [4]. Natural lithium consists of isotopes ^{6}Li and ^{7}Li with abundances 7.42 and 92.58%, respectively. The ^{7}Li(p,n)^{7}Be reaction was reviewed in 1960 by Gibbons and Newson [5]. Useful information on kinematics and technical aspects related to the use of ^{nat}Li may be found in [6]. Theoretically, using the R-matrix formalism, this reaction was studied in [6]-[8].

It should be noted that, in general, no source of neutrons is truly monoenergetic [9]. Even for a discrete transition, finite resolution of the accelerated protons, proton energy loss in the target and kinematics effects all contribute to a broadening of neutron energy. Secondary modes of reactions, which can compete significantly with the primary reaction modes at energies above their thresholds, produce either discrete groups or broad distributions of neutrons with energies differing from the primary-group energy. Until the yield of secondary neutrons is significantly smaller than the primary-group yield, it is usually possible to deal with the secondary neutrons by experimental methods (e.g., time-of-flight) or by the application of calculated corrections. When the yield of secondary neutrons begins to dominate the total yield, the reaction ceases to be useful for applications requiring monoenergetic neutrons. Nevertheless, even in this case, one still may consider LEDA as a useful source of neutrons for other applications, where “white” neutrons are suitable.

III. AN OVERVIEW OF AVAILABLE ^{7}Li(p,xn) DATA

Experimentally, this reaction was measured by several groups:

A) From threshold to about 8 MeV, by Meadows and Smith, using the Argonne Fast-Neutron Generator [9, 10];

B) From 10 to about 20 MeV, by Anderson et al., at Lawrence Radiation Laboratory [11], and from 4.3 to 26 MeV, by Poppe et al. (the same group) using EN tandem Van de Graaff accelerator (and AVF cyclotron, for $E_p > 15$ MeV) at Livermore [12]. Poppe at al. have been summarized in Ref. [12] practically all measurements of this reaction before 1976;

C) At 15, 20, and 30 MeV, by McNaughton et al., at the Croker Nuclear Laboratory [13];

D) By a number of other groups (see, e.g., [14]-[18]), at proton energies above 20 MeV.

Between 1.9– and 2.4–MeV bombarding energy, the neutrons are monoenergetic and the reaction cross section is large. Therefore the ^{7}Li(p,n)^{7}Be reaction has long been used as a source of neutrons (n_0) at these energies [5].

Above 2.4 MeV the first excited state of ^{7}Be at 0.43 MeV may be excited, producing a second group of neutrons (n_1). However, below 5 MeV the zero-degree yield of these low energy neutrons is less than about 10% of the ground-state yield, so that the usefulness of the reaction as a monoenergetic neutron source is only slightly impaired.

Above 3.68 MeV, the threshold for the three-body breakup reaction ^{7}Li(p,n^{3}He)^{4}He, neutrons from this mode contribute also to the total neutron yield. The zero-degree neutron spectra from this mode are very broad, of an evaporative-type form, and were measured up to $E_p = 7.7$ MeV by Meadows and Smith [10].

Above 7.06 MeV, the threshold for the reaction ^{7}Li(p,n)^{7}Be with excitation of the second excited state of ^{7}Be, neutrons from this mode (n_2) also begin to contribute to the total neutron yield, but this contribution is not significant [10]. Therefore, the usefulness of the ^{7}Li(p,n)^{7}Be reaction as a source of neutrons at energies above 5-7 MeV would depend on a particular application. Only a very good energy resolution would allow one to separate the substantial number of n_1 neutrons to obtain a monoenergetic source. However, if the application can tolerate including both n_0 and n_1 neutron groups, then the reaction has the favorable feature of use of a cheap solid target with a forward angle laboratory cross section approaching 7.4 mb/sr at $E_p = 15$ MeV and 14.5 mb/sr at $E_p = 20$ MeV (see Table II with our compilation of presently available experimental differential cross sections of neutrons measured at forward angles). It should be noted that although the neutron yield is large, the presence of low energy neutrons from different reaction modes may limit the usefulness of the ^{7}Li(p,n)^{7}Be reaction as a monoenergetic neutron source at proton energies above 10 MeV [12].

TABLE II

Compilation of measured laboratory differential cross sections at "zero" deg for the ^{7}Li(p,n)^{7}Be n_0 and n_1 (0.0 MeV and 0.43 MeV levels of ^{7}Be) reactions and the ratio of n_1 to n_0 neutrons (where available) as functions of proton kinetic bombarding energy, E_p, in MeV. Experimental errors are not shown if not given explicitly in tables or figures of original publications

E_p (MeV)	$(n_0 + n_1)$ Cross Section (mb/sr)	Ratio $R = n_1/n_0$	Reference	Cited angle of measurement
9.8	8.0 ± 1.0		[11]	0.
14.3	7.3 ± 0.5		[13]	0.
15.1	7.38	0.30	[12]	3.5
15.9	8.2	0.28	[12]	3.5
16.9	9.7	0.26	[12]	3.5
17.9	11.1	0.27	[12]	3.5
18.9	12.6	0.27	[12]	3.5
19.4	14.0 ± 0.9		[13]	0.
19.6	17.2 ± 1.5		[11]	0.
19.9	14.3	0.27	[12]	3.5
20.9	15.9	0.27	[12]	3.5
21.9	18.2	0.29	[12]	3.5
22.9	20.1	0.30	[12]	3.5
23.9	22.4	0.30	[12]	3.5
24.8	25.4 ± 4.9		[15]	0.
24.9	25.5	0.32	[12]	3.5
25.9	26.9	0.35	[12]	3.5
30.0	27.7		[19]	0.
29.4	35.5 ± 4.0		[20]	0.
29.6	27.0 ± 1.7		[13]	0.
30.0	27.7		[19]	0.
30.2	32.2 ± 3.0		[21]	0.
35.0	29.1 ± 2.9		[15]	0.
39.0	$33. \pm 6.$		[22]	0.
39.2	33.5 ± 3.0		[20]	0.
43.	35.0 ± 1.2		[18]	0.
45.0	31.6 ± 3.0		[15]	0.
48.	29.8 ± 1.0		[18]	0.
49.4	31.9 ± 2.5		[21]	0.
50.0	35.2 ± 3.5		[19]	0.
50.0	28.9 ± 2.9		[23]	0.
50.6	30.7 ± 3.0		[20]	0.
53.	33.4 ± 1.6		[18]	0.
58.	34.6 ± 1.2		[18]	0.
60.	$36. \pm 4.$		[22]	0.

Continuation of TABLE II

E_p (MeV)	(n_0+n_1) Cross Section (mb/sr)	Ratio $R=n_1/n_0$	Reference	Cited angle of measurement
63.	33.8 ± 1.2		[18]	0.
68.	33.9 ± 1.3		[18]	0.
78.	35.5 ± 1.6		[18]	0.
80.	$35.2 \pm 2.$		[17]	0.
87.	35.1 ± 2.2		[18]	0.
95.	33.2 ± 3.0		[24]	0.
100.	34.9 ± 3.2		[25]	0.
120.	35.3 ± 3.5		[26]	0.
120.	37.7 ± 3.1		[27]	0.
120.	35.1 ± 1.1		[17]	0.
135.	31.4 ± 3.1		[26]	0.
160.	33.8 ± 3.4		[26]	0.
160.	38.2 ± 3.4		[27]	0.
160.	35.4 ± 1.2		[17]	0.
200.	38.8 ± 2.7		[28]	0.
200.	38.0 ± 3.4		[27]	0.
200.	35.1 ± 1.0		[17]	0.
200.	32.4 ± 3.1		[25]	0.
300.	35.3 ± 2.4		[28]	0.
400.	35.8 ± 2.4		[28]	0.
494.	40.4 ± 1.6		[17]	0.
644.	42.7 ± 1.3		[17]	0.
795.	42.9 ± 1.1		[17]	0.

As mentioned above, the n_0 and n_1 neutron yields are strongly forward peaked. From Table II one can see that their measured cross section increases monotonically with increasing E_p. This is not true for the total neutron cross sections integrated over all emission angles, compiled in Table III and shown for $E_p < 26$ MeV in Fig. 1. One can see that in contrast with the zero degree differential cross section, the integrated cross section decreases monotonically above ~ 5 MeV, reflecting the onset of the strong forward peaking. Above $E_p = 7$ MeV, the total number of n_1 neutrons which leave ^{7}Be in the first-excited states is always greater than 25% of the number of n_0 neutrons which leave ^{7}Be in the ground state, reaching a maximum of about 55% at $E_p \sim 9$ MeV.

TABLE III

Compilation of measured laboratory angle integrated cross sections for the ^{7}Li(p,n)^{7}Be n_0 and n_1 (0.0 MeV and 0.43 MeV levels of ^{7}Be) reactions as a function of proton kinetic bombarding energy, E_p, in MeV. Experimental errors are not shown if not given explicitly in tables or figures of original publications

E_p (MeV)	(n_0+n_1)Cross Section (mb)	Reference	E_p (MeV)	(n_0+n_1)Cross Section (mb)	Reference
4.48	292.	[12]	39.5	18.03	[15]
4.68	316.	[12]	40.7	17.43	[15]
4.88	335.	[12]	44.7	16.44	[15]
5.48	304.5	[12]	60.1	12.00 ± 1.03	[16]
5.88	259.3	[12]	60.1	12.02 ± 1.02	[29]
6.88	178.5	[12]	62.0	11.28 ± 1.58	[16]
7.88	117.	[12]	69.4	10.78 ± 1.02	[16]
8.88	94.5	[12]	79.1	8.09 ± 0.71	[16]
9.88	65.2	[12]	80.0	7.96 ± 0.80	[29]
10.88	59.	[12]	88.9	7.46 ± 1.00	[16]
11.88	52.8	[12]	100.1	7.29 ± 0.77	[16]
15.1	37.4	[12]	119.4	5.29 ± 0.45	[16]
15.9	35.5	[12]	119.8	5.40 ± 0.17	[30]
16.9	33.95	[12]	120.1	4.88 ± 0.41	[29]
17.9	31.5	[12]	135.0	4.30 ± 0.41	[29]
18.9	32.	[12]	138.6	4.99 ± 0.43	[16]
19.9	29.6	[12]	143.9	4.97 ± 0.43	[16]
20.9	28.8	[12]	155.	3.5 ± 0.2	[31]
21.9	28.2	[12]	155.	3.8 ± 0.2	[32]
22.9	26.5	[12]	156.7	4.56 ± 0.42	[16]
23.9	26.19	[12]	160.1	3.77 ± 0.40	[29]
24.7	29.19	[15]	174.5	3.50 ± 0.36	[16]
24.9	26.3	[12]	190.0	3.01 ± 0.24	[29]
25.9	25.9	[12]	191.0	2.85 ± 0.19	[29]
27.3	26.06	[15]	199.1	3.46 ± 0.35	[16]
29.4	24.03	[15]	252.0	2.58 ± 0.30	[29]
29.9	24.12	[15]	301.0	1.73 ± 0.10	[29]
31.9	22.48	[15]	349.0	1.41 ± 0.26	[29]
34.5	20.84	[15]	400.0	1.47 ± 0.18	[29]
34.9	20.53	[15]	480.0	1.08 ± 0.07	[29]
36.6	19.46	[15]			

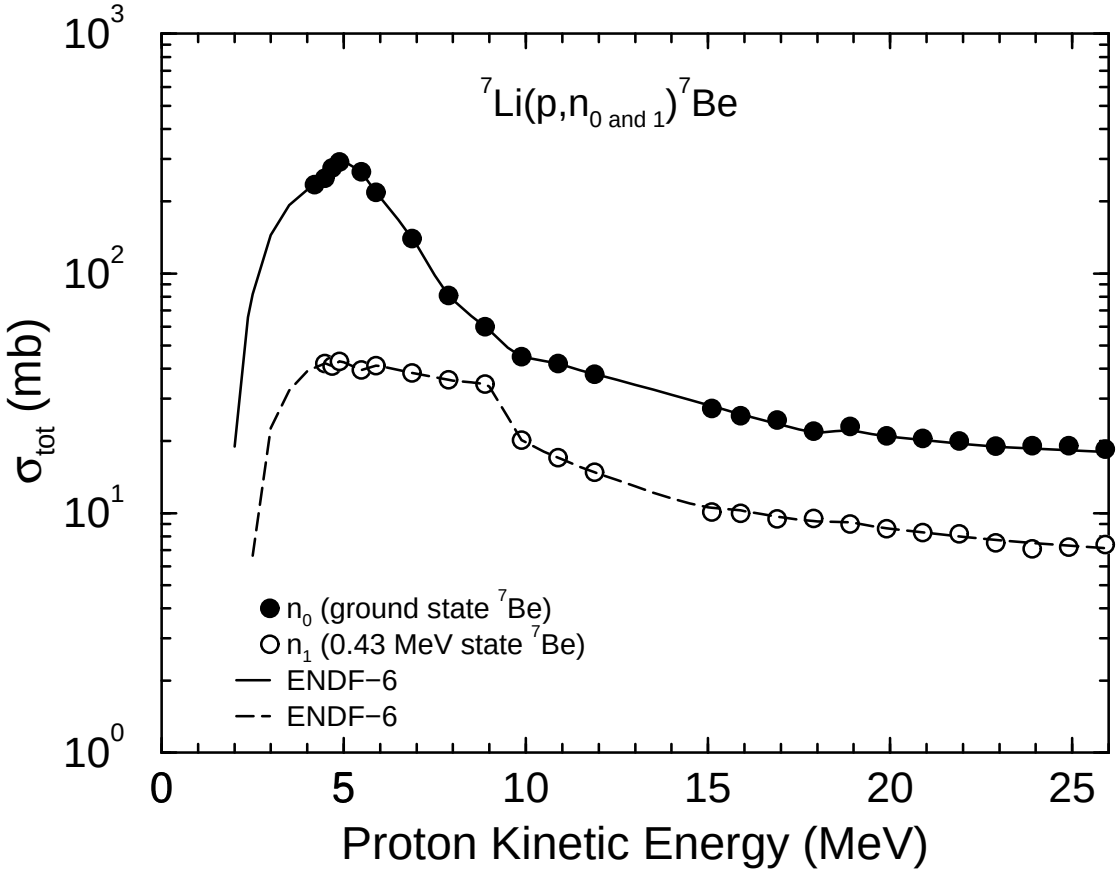

Figure 1: Measured total cross sections for the ^{7}Li(p,n$_0$)^{7}Be and ^{7}Li(p,n$_1$)^{7}Be reactions between 4 and 26 MeV [12] together with our evaluations in the ENDF-6 [33] format.

IV. EVALUATION METHODS

The production of an evaluated data library for proton reactions on lithium poses certain difficulties. In particular, nuclear model calculations based on statistical preequilibrium and equilibrium decay theories become unreliable for light target nuclei, where the nuclear levels are widely spaced. For this reason, one would like an evaluated data library that is based, as much as possible, on measured data.

We have therefore adopted the following approach. There are numerous measurements of the important ^{7}Li(p,n$_0$) and ^{7}Li(p,n$_1$) direct reactions populating the ground and first excited states of ^{7}Be, and we have used these experimental data for the cross sections and angular distributions in the evaluation. This is important because many aspects of the production of neutron sources via ^{7}Li(p,n) reactions involve use of the high-energy quasimonoenergetic n$_0$ and n$_1$ neutrons. To model the remaining cross section available for nuclear reactions, *i.e.* the overall reaction cross section minus these direct reaction cross sections, we use GNASH nuclear model calculations [34, 35].

Use of the GNASH calculations is expected to lead to some weaknesses in the evaluated data, because of the aforementioned difficulties in using a statistical model code. However, we note that the calculations do, at least, include certain important constraints such as energy, flux, angular momentum, and parity, conservation laws. Since the GNASH calculations make use of experimental nuclear levels information, they can also be expected to lead to emission spectra that correctly include peaks and gaps in the calculated energy-dependent spectra at the correct locations, *i.e.* peaks at energies where final states can be excited, and gaps where there are no final nuclear states available.

IV.A. Evaluation of n_0 and n_1 cross sections and angular distributions

The ^{7}Li(p,n$_0$) and ^{7}Li(p,n$_1$) evaluations were based upon measured data. The center-of-mass measured angular distributions of both the n$_0$ and n$_1$ neutrons were fitted using Legendre polynomials,

$$\frac{d\sigma_{c.m.}}{d\Omega} = \sum_{n=0}^{N} A_n P_n(cos\theta).$$

For proton incident energies up to 12 MeV, such Legendre fits have been published by Poppe *et al.*, and therefore we adopted their results (Fig. 5 of Ref. [12]).

At higher proton incident energies, we performed Legendre polynomial fits to measured angular distributions. For proton incident energies of 15.1, 15.9, 16.9, 17.9, 18.9, 19.9, 20.9, 22.0, 23.0, 24.0, 25.0, and 26 MeV, there are available measurements separately for n$_0$ and n$_1$ by Poppe *et al.* [12]. Above 26 MeV, there are fewer experimental data at only a limited number of incident energies and emission angles, and furthermore, only data for the sum of n$_0$ and n$_1$ are available. We used the measurements by Batty *et al.* [19] at 30 and 50 MeV, by Goulding *et al.* [30] at 119.8 MeV, and by Watson *et al.* [28] at 134.2 MeV. We fitted these data using for the ratio $R = n_1/n_0$ a fixed value of 0.35, as measured by Poppe *et al.* [12] at $E_p = 25.9MeV$, and smoothly interpolated/extrapolated the resulting Legendre coefficients up to $E_p = 150$ MeV.

As an example, Fig. 2 shows the sum of n$_0$ and n$_1$ measured total production cross section (for references, see Table III) as a function of proton kinetic energy, E_p, compared with our evaluation. One can see good agreement in the whole energy range up to 150 MeV.

IV.B. GNASH calculations

The latest version of the GNASH code has been described in Ref. [34], and its latest application in nuclear reaction evaluation work has been described in Ref. [36]. For this reason, here we provide only an overview of the models used in the calculations, concentrating on new features.

GNASH calculations of preequilibrium and Hauser-Feshbach decay require input parameter information describing the optical model transmission coefficients, nuclear level densities, gamma-ray strength functions, as well as nuclear level information for all the

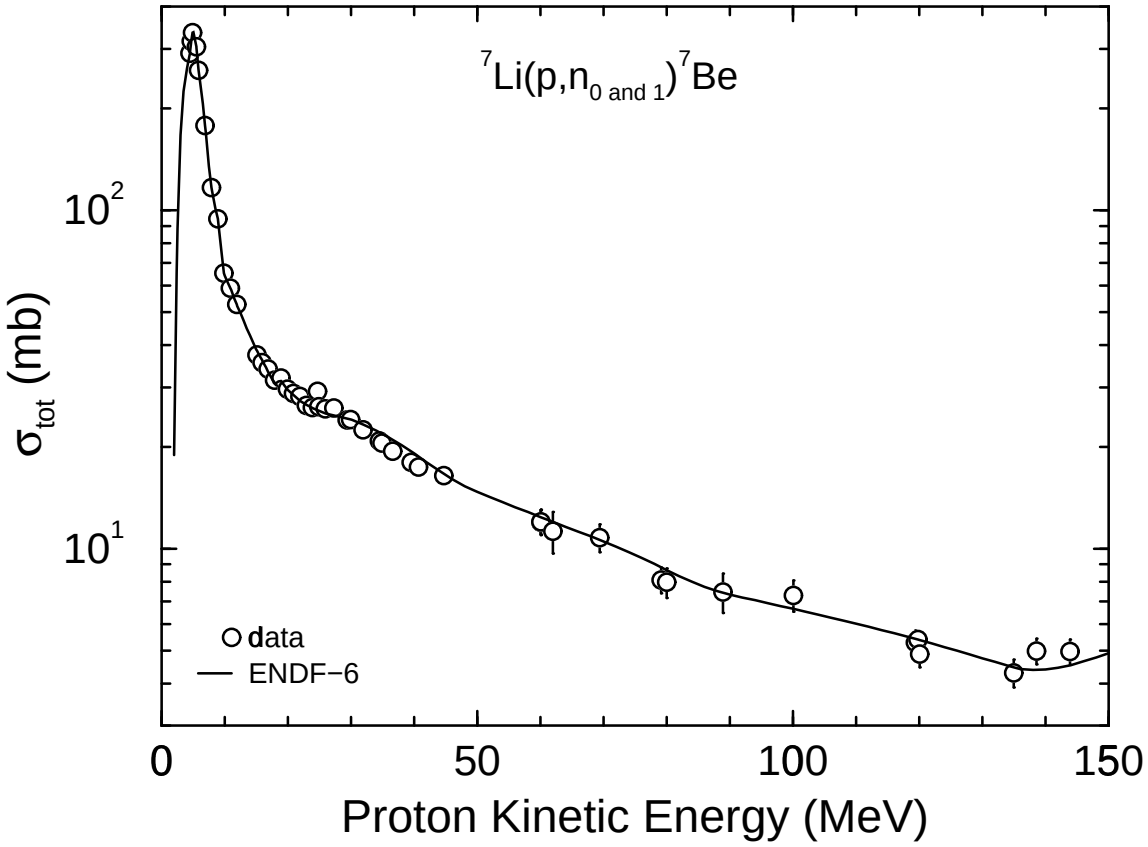

Figure 2: Comparison of the sum of measured [12, 15, 16, 26, 28] laboratory angle integrated cross sections for the ^{7}Li(p,n$_0$)^{7}Be and ^{7}Li(p,n$_1$)^{7}Be reactions (for details, see Table III) with our evaluation in the ENDF-6 format.

nuclei that can be populated in the reaction. For most of these quantities, we used default parameter information, as described in Ref. [36]. Below, we provide information on the optical model we used for ^{7}Li.

Although the appropriateness of an optical potential for nucleon scattering on a light nucleus such as lithium is questionable, we have, for pragmatic reasons, made use of a relativistic potential for ^{6}Li published by Chiba *et al.* [37]. This potential was shown to provide a surprisingly good representation of available elastic scattering and total cross section data, for energies up to a few hundred MeV [37]. We converted this neutron potential for use on ^{7}Li by making small isospin corrections, and produced a version for proton scattering by including Coulomb correction terms. The modified potentials resulted in a calculated total neutron cross section that accounted for measured data fairly well. The calculated proton reaction cross section was also in good agreement with measurements (see Fig. 3).

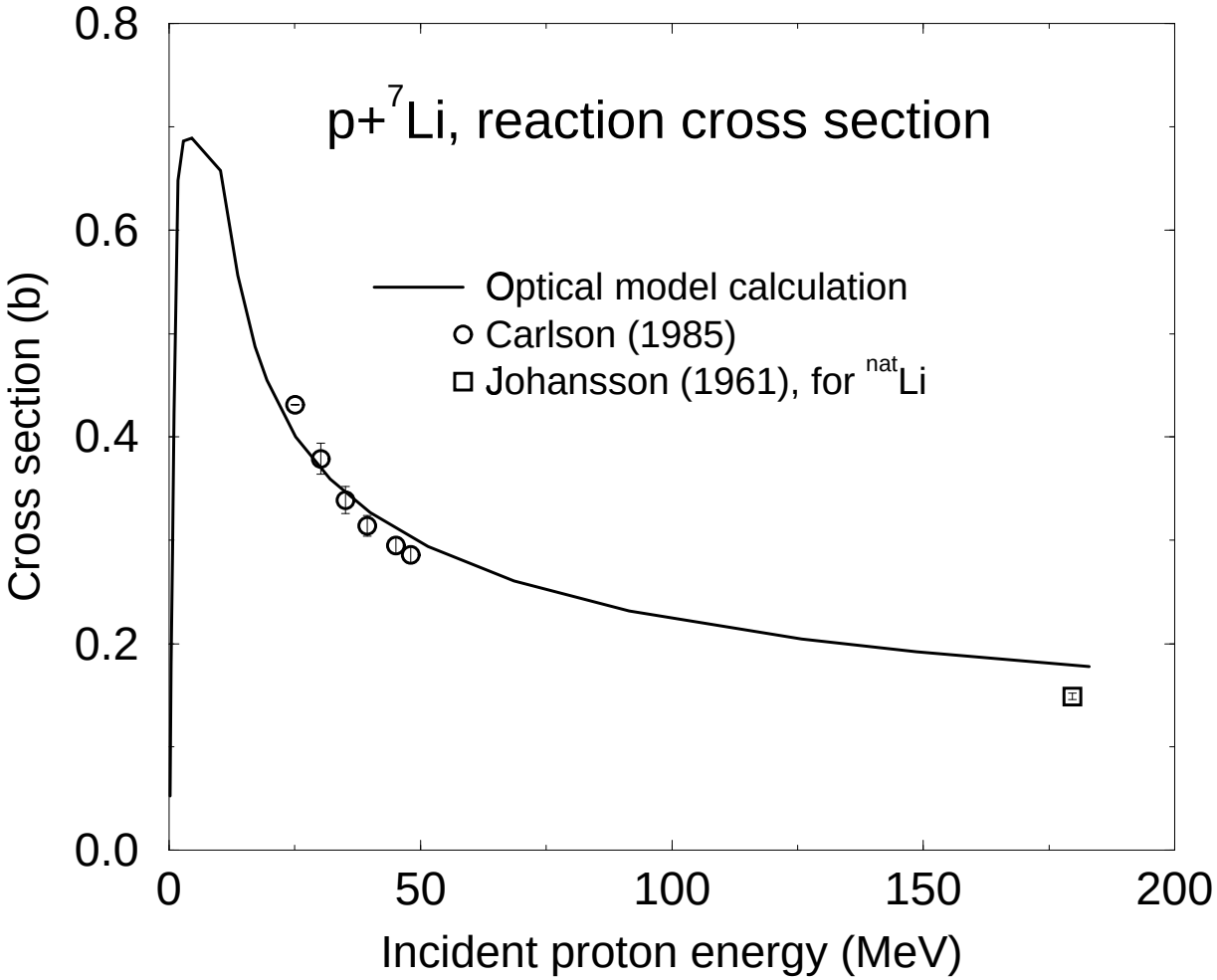

Figure 3: Proton reaction cross section of ^{7}Li. The solid curve shows values calculated with the optical model by Chiba *et al.* [37] modified here as described in Section IV.B. Experimental data are from Refs. [38, 39].

Since the GNASH code includes n_0 and n_1 neutron emission contributions from compound nucleus and preequilibrium decay, these cross sections had to be ignored since, in our evaluation, they are based on measurements. Therefore we wrote a utility code that takes a GNASH output, modifies the n_0 and n_1 neutron emission cross sections to zero, and in the evaluated file introduces the cross sections based on experiment as described in Sec. IV A above.

Examples of the ^{7}Li(p,xn) calculated zero-degree double-differential cross sections of neutrons are shown in Fig. 4, compared with measurements. Solid lines show the results from the GNASH calculations; Dashed-lines show the n_0 and n_1 contributions (evaluated from the measurements). Comparisons are made with $E_p = 15$, 20, and 30 MeV data of McNaughton et al. [13], $E_p = 40$ MeV data of Jungerman et al. [14], and at $E_p = 55$, 90, and 140 MeV data of Byrd and Sailor [40]. In these figures, in addition to the highest-energy peak due to n_0 and n_1 neutrons, several lower-energy peaks due to n_2 and n_3 neutrons, representing the population of the 4.55- and 6.51-MeV states in ^{7}Be are evident (see also, e.g., Fig. 2 in Poppe et al. [12], where even the peaks by n_4 and n_5, representing the population of the 7.19- and 10.79-MeV states in ^{7}Be are clearly observed).

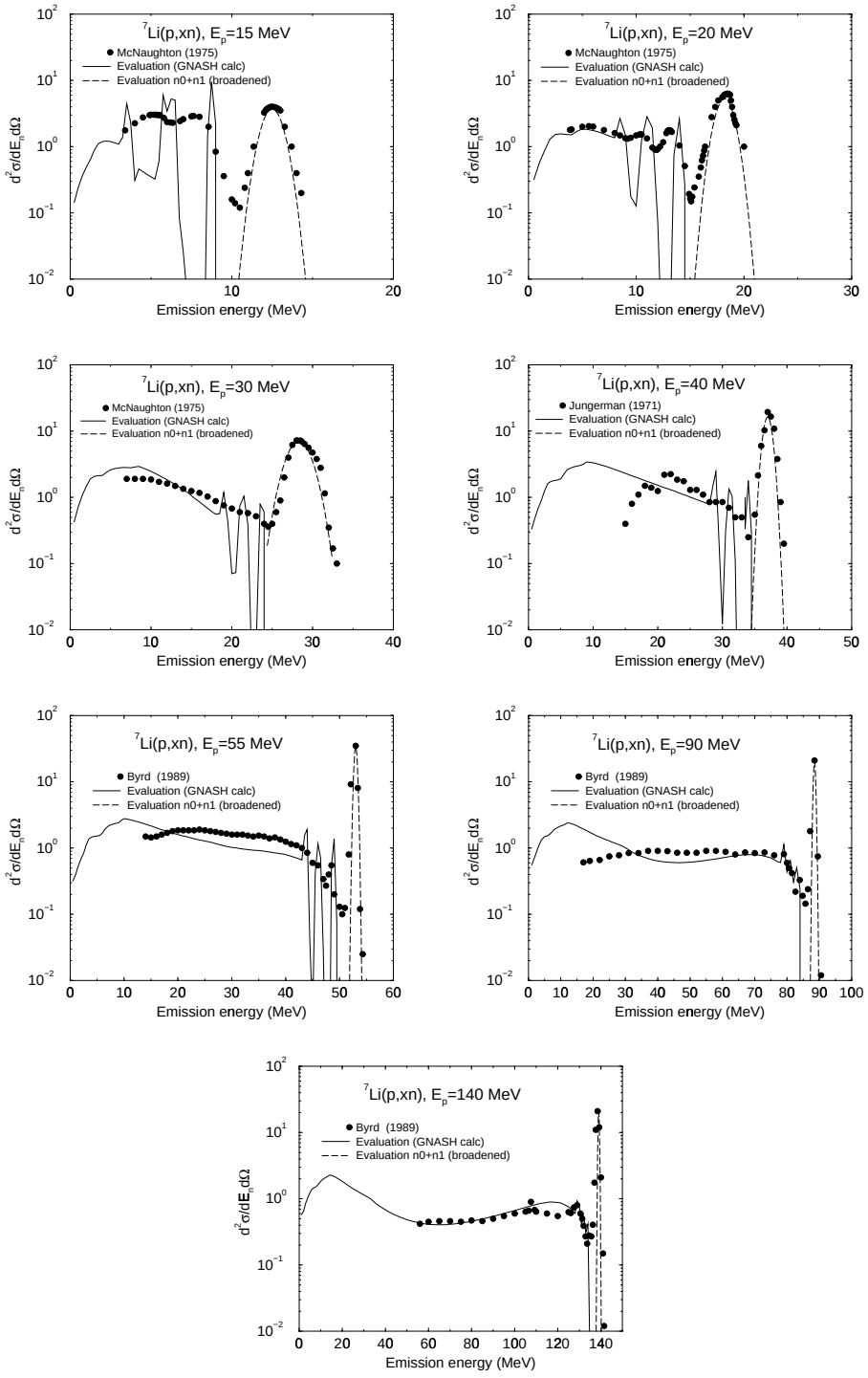

Figure 4: Zero degree neutron emission from the ^{7}Li(p,xn) reaction. Solid lines show the results from the GNASH calculations, dashed lined show n_0 and n_1 contributions evaluated from the measurements. The GNASH-calculated spectra have not been broaded using the experimental resolution. Data are from Refs. [13, 14, 40].

We emphasize that the GNASH results shown in Fig. 4 have not been broadened to account for the experimental detector resolution. This explains why peaks and dips are observed in the calculated energy-dependent spectra, but are not seen so prominantly in the experimental data. Overall, it is evident that the evaluation accurately represents the n_0 and n_1 neutrons, as it should since it is based on the experimental data. The lower-energy neutrons from the GNASH calculation agree with the measurements less well, but it is hoped that the accuracy obtained is sufficient for LEDA design calculations.

V. ENDF Data

In this section we show some graphical representations of the evaluated ENDF data. These figures help illustrate certain features of the evaluation. The figures shown here are a small subset of figures produced automatically by the NJOY code [41]. The full set of figures can be viewed on the T-2 WWW site, by first going to http://t2.lanl.gov/data/he.html, registering, and then clicking on premade plots in Postscript format for protons (http://t2.lanl.gov/data/p-ps/).

Figure 5 shows the proton elastic scattering angular distribution for incident energies up to 150 MeV. The increased forward-peaking with increasing incident energy is evident. Figure 6 shows the angular distributions, reconstructed from the ENDF Legendre coefficients, for the n_0 and n_1 emitted neutrons.

Four separate figures are combined together in figure 7. On the top left, the overall cross sections for the n_0, and n_1 reactions are shown, as is also the "remaining" cross section, designated as MT=5, that is used in the GNASH calculations. The sum of all these cross sections is the reaction cross section as shown in Fig. 3.

In Fig. 7, top right, the inclusive production cross sections are shown for the light ejectiles. Note that, unlike for reactions on heavier nuclei, these do not keep increasing with incident energy up to 150 MeV, but instead become approximately constant above 40 MeV. This energy corresponds, approximately, to the total binding energy of ^{7}Li, and therefore above this energy it is not possible to obtain additional particle production by increasing the incident energy.

In Fig. 8 lower-left, a perspective plot is shown of the angle-integrated neutron emission spectra obtained from GNASH, as a function of incident energy. The increasing role of preequilibrium high-energy neutron emission is seen as the incident energy increases. Finally, in Fig. 7 lower-right the total heating (MeV/collision) is shown as a function of incident energy. This includes energy transferred to all secondary charged-particles, except protons (since this is the projectile, and it is therefore assumed that a transport calculation will always be explicitly tracking the secondary protons).

VI. SUMMARY AND FUTURE WORK

Our new evaluation for protons on ^{7}Li is available in the ENDF-6 format for use in radiation transport calculations. By using and testing these data in simulations of thick and thin lithium targets, we hope to obtain feedback on possible improvements that are needed.

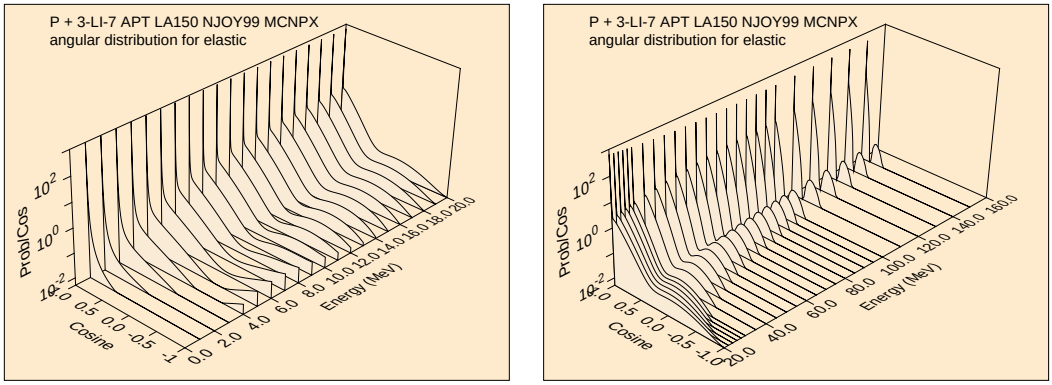

Figure 5: Proton elastic scattering angular distribution of ^{7}Li at different incident energies up to 150 MeV.

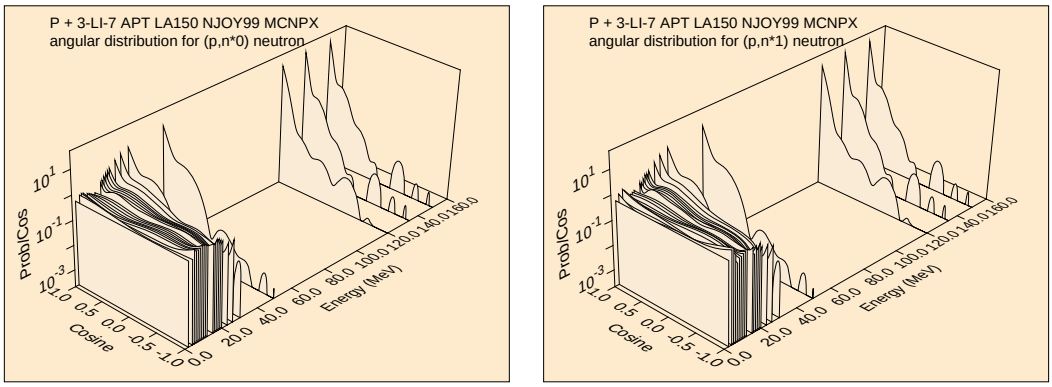

Figure 6: Angular distributions for n_0 and n_1 neutrons from p + ^{7}Li interactions at different incident energies up to 150 MeV.

For completeness, we list here a couple of areas where we know there is room for improvement. The first point discussed below emphasizes weaknesses in the ENDF evaluation that may be problematic for simulations above 30 MeV.

Firstly, as discussed in this report, the angular distributions of the high-energy n_0 and n_1 protons were represented in the ENDF file using Legendre coefficients. However, the scarcity of measured data at various angles in the measured angular distributions led to difficulties in obtaining accurate Legendre representations. Furthermore, at higher incident energies (above 30 MeV), the data at forward angles often showed an extreme discontinuous increase in cross section at zero-degrees. This was impossible to fit accurately, and our resulting Legendre fits therefore underpredicted the zero-degree data above 30 MeV, by up to a factor of two. To solve this problem, it may be necessary to abandon the use of a Legendre representation, and instead use tabulated representations of the angular distributions.

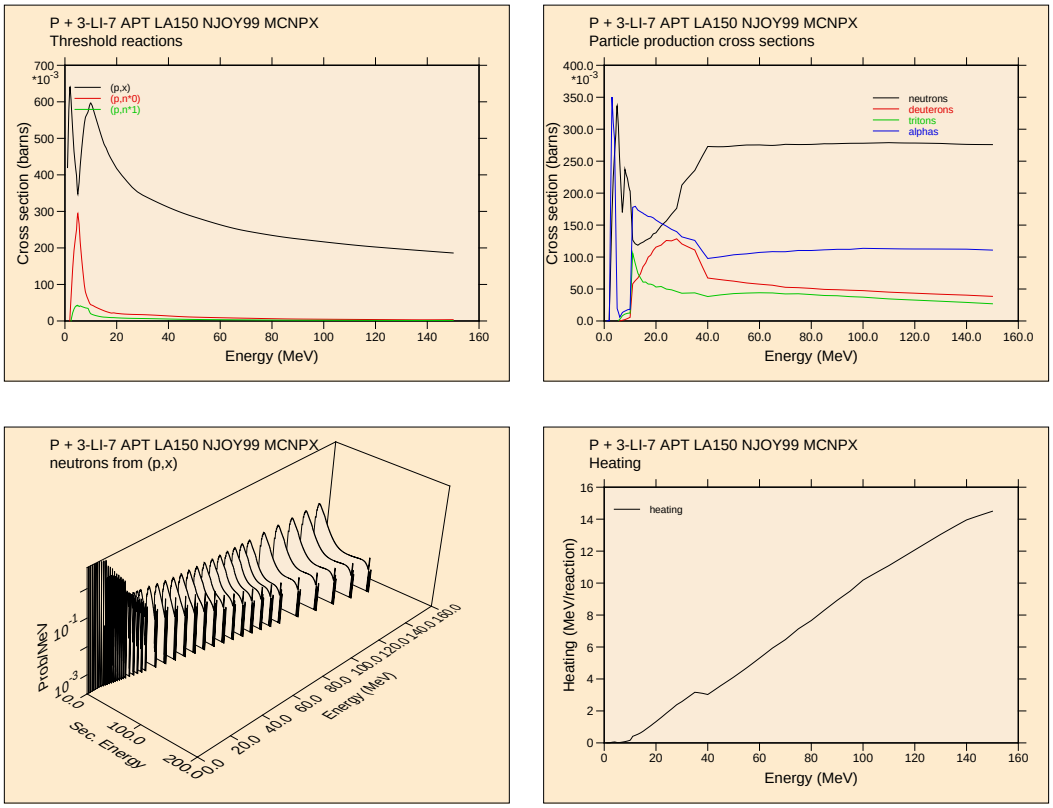

Figure 7: Different chanel cross sections, neutron angle-integrated energy spectra, and heating (MeV/collision) as functions of incident energy for p + ^{7}Li interactions, as indicated.

Secondly, our analysis was not developed to include an accurate treatment of gamma-ray production, but instead focussed on neutron emission. Indeed, the nuclear level information in the GNASH calculations describing the decay of excited states by gamma-ray emission was not carefully checked. Therefore, if gamma-ray emission becomes of concern in LEDA target design studies, an upgrade to this evaluation may be needed.

ACKNOWLEDGMENTS

The authors are grateful to J. L. Ullmann and W. B. Wilson for useful discussions and information.

This study was supported by the U. S. Department of Energy.

REFERENCES

[1] J. C. BROWNE, J. L. ANDERSON, M. W. CAPPIELLO, G. P. LAWRENCE, and P. W. LISOWSKI, "Status of the Accelerator Production of Tritium (APT) Project," *Proc. APT Symp. The Savannah River Accelerator Project and Complementary Spallation Neutron Sources,* University of South Carolina, Columbia, USA, May 14-15, 1996, p. 14, F. T. AVIGNONE and T. A. GABRIEL, Eds., World Scientific, Singapore, (1998).

[2] *ED&D Monthly Report, October, 1999*, LA-UR 99-6201, Los Alamos National Laboratory (1999).

[3] M. DROSG, "Sources of Variable Energy Monoenergetic Neutrons for Fusion-Related Applications," *Nucl. Sci. Eng.*, **106**, 279 (1990).

[4] M. L. ROUSH, L. A. WEST, and J. B. MARION, "Precision Determinations of Nuclear Reaction Calibration Energies by Velocity Measurements," *Nucl. Phys. A*, **147**, 235 (1970).

[5] J. H. GIBBONS and H. W. NEWSON, "The ^{7}Li(p,n)^{7}Be Reaction," *Fast Neutron Physics,* Vol. 1, J. B. MARION and J. L. FOWLER, Eds., Interscience, New York (1960).

[6] J. H. LANGSDORF, Jr., J. E. MONAHAN, and W. A. REARDON, "A Tabulation of Neutron Energies from Monoenergetic Protons on Lithium," ANL-5219, Argonne National Laboratory (Jan. 1954).

[7] S. G. BUCCINO, C. E. HOLLANDSWORTH, and P. R. BEVINGTON, "Neutron Yields from the ^{7}Li(p,n$'$)^{7}Be* Reaction Near Threshold," *Nucl. Phys.*, **53**, 375 (1964).

[8] A. BERGSTROM, S. SCHWARZ, L. G. STROMBERG, and L. WALLIN, "Angular Distributions of Neutrons from the ^{7}Li(p,n)^{7}Be Reaction Near Threshold," *Arkiv for Fysik*, **34**, 153 (1967).

[9] J. W. MEADOWS and D. L. SMITH, "Neutron Source Investigations in Support of the Cross Section Program at the Argonne Fast-Neutron Generator," ANL/NDM-53, Argonne National Laboratory (May 1980).

[10] J. W. MEADOWS and D. L. SMITH, "Neutrons from Proton Bombardment of Natural Lithium," ANL-7938, Argonne National Laboratory (June 1972).

[11] J. D. ANDERSON, C. WONG, and V. A. MADSEN, "Charge Exchange Part of the Effective Two-Body Interaction," *Phys. Rev. Lett.*, **24**, 1074 (1970).

[12] C. H. POPPE, J. D. ANDERSON, J. C. DAVIS, S. M. GRIMES, and C. WONG, "Cross Sections for the ^{7}Li(p,n)^{7}Be Reaction Between 4.2 and 26 MeV," *Phys. Rev. C*, **14**, 438 (1976).

[13] M. W. McNAUGHTON, N. S. P. KING, F. P. BRADY, J. L. ROMERO, and T. S. SUBRAMANIAN, "Measurements of ^{7}Li(p,n) and ^{9}Be(p,n) Cross Sections at 15, 20, and 30 MeV," *Nucl. Instr. Meth.*, **130**, 555 (1975).

[14] J. A. JUNGERMAN, F. P. BRADY, W. J. KNOX, T. MONTGOMERY, M. R. McGIE, J. L. ROMERO, and Y. ISHIZAKI, "Production of Medium-Energy Neutrons from Proton Bombardment of Light Elements," *Nucl. Instr. Meth.*, **94**, 421 (1971).

[15] S. D. SCHERY, L. E. YOUNG, R. R. DOERING, S. M. AUSTIN, and R. K. BHOWMIK, "Activation and Angular Distribution Measurements of ^{7}Li(p,n)^{7}Be ($0.0 + 0.429$ MeV) for $E_p = 25 - 45$ MeV: A Technique for Absolute Neutron Yield Determination," *Nucl. Instr. Meth.*, **147**, 399 (1977).

[16] T. E. WARD, C. C. FOSTER, G. E. WALKER, J. RAPAPORT, and C. A. GOULDING, "$1/E$ Dependence of the ^{7}Li(p,n)^{7}Be (g.s.$+0.43$ MeV) Total Reaction Cross Section," *Phys. Rev. C*, **25**, 762 (1982).

[17] T. N. TADDEUCCI, W. P. ALFORD, M. BARLETT, R. C. BYRD, T. A. CAREY, D. E. CISKOWSKI, C. C. FOSTER, C. GAARDE, C. D. GOODMAN, C. A. GOULDING, J. B. McCLELLAND, D. PROUT, J. RAPAPORT, L. J. RYBARCYK, W. C. SAILOR, E. SUGARBAKER, and C. A. WHITTEN, Jr., "Zero-Degree Cross Sections for the ^{7}Li(p,n)^{7}Be (g.s.$+0.43$ – MeV) Reaction in the Energy Range 80-795 MeV," *Phys. Rev. C*, **41**, 2548 (1990).

[18] M. BABA, Y. NAUCHI, T. IWASAKI, T. KIYOSUMI, M. YOHIOKA, S. MATSUYAMA, N. HIRAKAWA, T. NAKAMURA, Su. TANAKA, S. MEIGO, H. NAKASHIMA, Sh. TANAKA, N. NAKAO, "Characterization of 40-90 MeV ^{7}Li(p,n) Neutron Source at TIARA Using a Proton Recoil Telescope and a TOF Method," *Nucl. Instr. Meth. A*, **428**, 454 (1999).

[19] C. J. BATTY, B. E. BONNER, A. I. KILVINGTON, C. TSCHALÄR, and L. E. WILLIAMS, "Intermediate Energy Neutron Sources," *Nucl. Instrum. Methods*, **68**, 273 (1969).

[20] J. L. ROMERO, F. P. BRADY, J. A. JUNGERMAN, "Production of Medium-Energy Neutrons from Proton Bombardment of Light Elements Using Revised Neutron-Proton Differential Cross Sections," *Nucl. Instrum. Methods*, **134**, 537 (1976).

[21] C. J. BATTY, B. E. BONNER, E. FRIEDMAN, C. TSCHALÄR, L. E. WILLIAMS, A. S. CLOUGH, and J. B. HUNT, "The ^{6}Li(p,n)^{6}Be and ^{7}Li(p,n)^{7}Be Reactions at Intermediate Proton Energies," *Nucl. Phys. A*, **120**, 297 (1968).

[22] J. L. WACHTER, R. T. SANTORO, T. A. LOVE, and W. ZOBEL, "Fast Forward Neutron Production in the ^{7}Li(p,n)^{7}Be Reaction for 41- and 64-MeV Protons," *Nucl. Instrum. Methods,* **113**, 185 (1973).

[23] M. BOSMAN, P. LELEUX, P. LIPNIK, P. MACQ, J. P. MEULDERS, R. PETIT, C. PIRART, and G. VALENDUC, "Neutron Beam Facility at the Louvain-la-Neuve Isochronous Cyclotron; Cross Sections for Fast Neutron Production," *Nucl. Instrum. Methods,* **148**, 363 (1978).

[24] A. LANGSFORD, PR/NP7, p. 28, Atomic Energy Research Establishment (Harwell) (1964).

[25] R. POURANG, Ph.D. Thesis, Kent State University (1989).

[26] J. W. WATSON, B. D. ANDERSON, A. R. BALDWIN, C. LEBO, B. FLANDERS, W. PAIRSUWAN, R. MADEY, and C. C. FOSTER, "A Comparison of Methods for Determining Neutron Detector Efficiencies at Medium Energies," *Nucl. Instrum. Methods,* **215**, 413 (1983).

[27] T. N. TADDEUCCI, C. A. GOULDING, T. A. CAREY, R. C. BYRD, C. D. GOODMAN, C. GAARDE, J. LARSEN, D. HOREN, J. RAPAPORT, and E. SUGARBAKER, "The (n,p) Reaction as a Probe of Beta Decay Strength," *Nucl. Phys. A*, **469**, 125 (1987).

[28] J. W. WATSON, R. POURANG, R. ABEGG, W. P. ALFORD, A. CELLER, S. ElKATEB, D. FREKERS, O. HÄUSSER, R. HELMER, R. HENDERSON, K. HICKS, K. P. JACKSON R. G. JEPPESEN, C. A. MILLER, M. VETTERLI, S. YEN, and C. D. ZAFIRATOS, "^{7}Li(p,n)^{7}Be and ^{12}C(p,n)^{12}N Reactions at 200, 300, and 400 MeV," *Phys. Rev. C*, **40**, 22 (1989).

[29] J. D'AURIA, M. DOMBSKY, L. MORITZ, T. RUTH, G. SHEFFER, T. E. WARD, C. C. FOSTER, J. W. WATSON, B. D. ANDERSON, and J. RAPAPORT, "Activation Measurements of the ^{7}Li(p,n)^{7}Be Reaction from 60-480 MeV," *Phys. Rev. C,* **30**, 1999 (1984).

[30] C. A. GOULDING, M. B. GREENFIELD, C. C. FOSTER, T. E. WARD, J. RAPAPORT, D. E. BAINUM, and C. D. GOODMAN, "Comparison of the ^{12}C(p,n)^{12}N and ^{12}C(p,p′) Reactions at $E_p = 62$ and 120 MeV," *Nucl. Phys. A*, **331** 29 (1979).

[31] L. VALENTIN, G. ALBOUY, J. P. COHEN, and M. GUSAKOW, "Reactions Induites par des Protons de 155 MeV sur des Noyaux Legers," *Phys. Lett.*, **7**, 163 (1963).

[32] L. VALENTIN, "Réactions (p,n) et (p,pn) Induites à Moyenne Énergie sur des Noyaux Légers," *Nucl. Phys.*, **62**, 81 (1965).

[33] V. McLANE, "ENDF-102 Data Formats and Procedures for the Evaluated Nuclear Data File ENDF-6," BNL-NCS-44945, Rev. 2/97, Brookhaven National Laboratory, National Nuclear Data Center (1997).

[34] P. G. YOUNG, E. D. ARTHUR, and M. B. CHADWICK, "Comprehensive Nuclear Model Calculations: Theory and Use of the GNASH Code," *Proc. IAEA Workshop on Nuclear Reaction Data and Nuclear Reactors — Physics, Design, and Safety*, Trieste, Italy, April 15 – May 17, 1996, p. 227, A. GANDINI and G. REFFO, Eds., World Scientific Publishing, Ltd., Singapore (1998).

[35] P. G. YOUNG, E. D. ARTHUR, and M. B. CHADWICK, "Comprehensive Nuclear Model Calculations: Introduction to the Theory and Use of the GNASH Code," LA-12343-MS, Los Alamos National Laboratory (1992).

[36] M. B. CHADWICK, P. G. YOUNG, S. CHIBA, S. C. FRANKLE, G. M. HALE, H. G. HUGHES, A. J. KONING, R. C. LITTLE, R. E. MacFARLANE, R. E. PRAEL, and L. S. WATERS, "Cross-Section Evaluations to 150 MeV for Accelerator-Driven Systems and Implementation in MCNPX," *Nucl. Sci. Eng.*, **131**, 293 (1999).

[37] S. CHIBA, K. TOGASAKI, M. IBARAKI, M. BABA, S. MATSUYAMA, N. HIRAKAWA, K. SHIBATA, O. IWAMOMOTO, A. J. KONING, G. M. HALE, and M. B. CHADWICK, "Measurements and Theoretical Analysis of Neutron Elastic Scattering and Inelastic Reactions Leading to a Three-Body Final State for ^{6}Li at 10 to 20 MeV," *Phys. Rev. C*, **58**, 2205 (1998).

[38] R. F. CARLSON, A. J. COX, T. N. NASR, M. S. DE JONG, D. L. GINTHER, D. K. HASELL, A. M. SOURKES, W. T. H. VAN OERS, and D. J. MARGAZIOTIS, "Measurements of Proton Total Reaction Cross Sections for ^{6}Li, ^{7}Li, ^{14}N, ^{20}Ne, and ^{40}Ar Between 23 and 49 MeV," *Nucl. Phys. A*, **445**, 57 (1985).

[39] A. JOHANSSON, U. SVANBERG, and O. SUNDBERG, "Total Nuclear Reaction Cross Sections for 180 MeV Protons," *Arkin für Fisik*, **19**, 527 (1961).

[40] R. C. BYRD and W. C. SAILOR, "Neutron Detection Efficiency for NE213 and BC501 Scintilators at Energies Between 25 and 200 MeV," *Nucl. Instrum. Methods A*, **274**, 494 (1989).

[41] R. E. MacFARLANE, "Recent Progress on NJOY," LA-UR-96-4688, Los Alamos National Laboratory (1996); the last version of the code, NJOY99, is described on the Web page at hppt://t2.lanl.gov/codes/codes.html.